Removal of Hg^{2+} From Desulfurization Wastewater By Tannin-Immobilized Graphene Oxide

Heng Chen
Southeast University
Fengjun Liu
Southeast University
Chenjian Cai
Southeast University
Hao Wu
Nanjing Normal University
Linjun Yang (ylj@seu.edu.cn)
Southeast University

Research Article

Keywords: Mercury, Desulfurization wastewater, GO, Tannin, Removal efficiency

Posted Date: July 13th, 2021

DOI: https://doi.org/10.21203/rs.3.rs-599443/v1

Version of Record: A version of this preprint was published at Environmental Science and Pollution Research on October 22nd, 2021. See the published version at https://doi.org/10.1007/s11356-021-16993-7.

Abstract

A novel adsorbent by immobilizing tannic acid (TA) on graphene oxide (GO) was proposed and used to remove Hg^{2+} from desulfurization wastewater. The morphology and physic-chemical property of tannin-immobilized graphene oxide (TAIGO) was characterized by Scanning electron microscopy (SEM), Atomic Force Microscope (AFM), and Fourier transform infrared spectroscopy (FTIR). The characterization results showed that the TA was immobilized on the GO successfully, and new functional groups were introduced on TAIGO. The effect of contact time, adsorbent dose, pH, and ion components on removal efficiency were evaluated. It was found that the adsorption process would complete within 15 min, and a higher removal efficiency could be obtained on the increased adsorbent dosage. The pH value would affect the protonation process of TAIGO and the form of Hg^{2+} in the wastewater. The high-concertation Cl^- and SO_3^{2-} would hinder the absorption performance, while SO_4^{2-} and cations had a negligible impact. Besides, an excellent economic benefit of TAIGO was achieved in the regeneration performance evaluation experiment, and removal efficiency of was 88% remained after three recycles. Most importantly, the TAIGO exhibited a better adsorption performance and economic benefit than GO and TA. The adsorption process was fitted with the pseudo-second-order kinetic model(R=0.9995), and the adsorption of TAIGO for Hg^{2+} was mainly relies on the functional groups on GO and the chelation reaction between TA and Hg^{2+}. These facts indicated that the TAIGO was a low-cost and high removal of Hg^{2+} efficiency adsorbent, which could be further used in the practical desulfurization wastewater.

Introduction

The Wet Flue Gas Desulfurization (WFGD) system has been widely used for SO_X treatment, and it also has a synergistic effect to remove Hg^{2+} from the flue gas (Zhang et al., 2017). It was reported that around 90% Hg^{2+} could be captured by the WFGD system and entered into desulfurization slurry (Krzyżyńska et al., 2020). However, the excessed heavy metals and Cl^- accumulated in the slurry may lead to the deterioration of desulfurization slurry quality, which was a disadvantage for the desulfurization process. Thus, the WFGD system would regularly discharge desulfurization wastewater and supply fresh water to keep the quality of desulfurization slurry (Zheng et al., 2019). The coal-fired power plant would generate a large amount of desulfurization wastewater, which would bring great stress on the environment (Zheng et al., 2020). Therefore, it is necessary to treat the Hg^{2+} in desulfurization wastewater. At present, the conventional method for desulfurization wastewater treatment is to use the triplet tank technology, and the heavy metals could be removed by TMT15 and DTCR (Jan et al., 2018). TMT15 is a favoured organic sulfide reagent, which could co-precipitate the heavy metals. However, because of its toxicity, it cannot make water quality conform to strict regulation. The adsorption method was regarded as an effective, economical and environmentally friendly way to treat the Hg^{2+} in desulfurization wastewater (Hsu et al., 2020; Taurozzi et al., 2020).

Graphene oxide (GO), a crystalline allotrope of sp^2-bonded carbon with honeycomb-shaped two-dimensional nanomaterial, has attracted great concern (Yang et al., 2020). Own to its excellent

mechanical and chemical properties, the GO has been applied in many fields (Mounir et al., 2021; Ebrahim et al., 2020). Besides, due to abound functional groups and great specific surface area (2630 m^2/g), the GO shows considerable potential in water treatment (Li et al., 2020; Sun et al., 2020). A lot of researches have been done to investigate the GO adsorption capacity in Hg^{2+} containing wastewater. Bao et al. (2013) investigated the removal performance of magnetite/graphene oxide (MGO) for Hg^{2+}, and the result shows that the adsorption capacity of MGO was 289.9 mg/g. Palanive (Palanivel et al., 2020) reported that the Hg^{2+} ions could be effective removed by GO-based absorbate. However, the GO's high price causes difficulty in treating the massive emission of desulfurization wastewater from powerplant (Powell et al., 2015). Thus, it is meaningful to modify the GO to reduce the total cost.

Tannic acid (TA), a low-cost biomass reagent that could be extracted from plants, has been reported as excellent adsorption towards heavy metals due to the abundance of adjacent phenolic hydroxyls (Yue et al., 2019). Taksitta et al. (2020) provided a tannin-based absorbent to remove Cu, Cd and Pb from wastewater, and the results showed that the heavy metals could be removed effectively. However, the TA exhibited good water-soluble propriety. That is, it cannot be collected from wastewater for reusing, which may affect its further utilization. Thus, the various matrix was used to immobilized tannic acid to overcome this disadvantage. Fan et al. (2019) fabricated the tannin-based absorbent, which immobilized on $Fe_3O_4@SiO_2$, and the $Fe_3O_4@SiO_2@PT$ could be facilely separate from wastewaters after the adsorption process. Huang et al. (2009) created the tannin immobilized on the collagen fiber, and the adsorption experiments were carried out to investigated the adsorption performance for Hg^{2+}. Wang et al. (2019) reported a graphene oxide-based material, which crosslinked with persimmon tannins through the desired groups for methylene blue removal. It can be inferred that tannin-immobilized graphene oxide (TAIGO) might be a feasible adsorbent, which can improve the adsorption performance and overcome the water-soluble propriety of TA, and the falling cost was favored.

In this study, the TAIGO was fabricated, and the adsorption performance of Hg^{2+} was evaluated in the desulfurization wastewater. The effect of contacted time, TAIGO dosage, pH and ion component on removal efficiency was investigated. Besides, the possible adsorption mechanism was proposed based on the adsorption kinetics and the experimental results. Furthermore, the regeneration experiments were also conducted to investigate the recyclability performance of TAIGO.

Experimental And Methods

2.1 Materials

The reagents sulfuric acid (H_2SO_4), Hydrogen peroxide (H_2O_2), potassium permanganate ($KMnO_4$), hydrochloric acid (HCl), nitric acid (HNO_3), sodium sulphite (Na_2SO_3) and Tannic acid (TA) were purchased from Nanjing Chemical Reagent Limited Ltd. The graphite was obtained from Sinopharm Chemical Reagent. The desulfurization wastewater was collected from two different coal-fired power plants in Nanjing. The compositions of desulfurization wastewater were listed in Table 1.

Table 1
The composition of desulfurization wastewater.

Compositions	desulfurization wastewater A	desulfurization wastewater B
pH	6.3	6.5
SS (%)	2	3
Hg^{2+}(mg/L)	0.4	0.5
K^{+}(mg/L)	100	1400
Na^{+}(mg/L)	90	3900
Ca^{2+}(mg/L)	50	500
Mg^{2+}(mg/L)	7800	11000
Cl^{-}(mg/L)	3500	13000
SO_4^{2+}(mg/L)	16000	18000
SO_3^{2+}(mg/L)	540	1350

2.2 Immobilization of tannic acid on GO

In this paper, the GO was prepared via the Hummers method, which was mainly divided into three stages: low temperature, medium temperature, and high temperature process. Firstly, the graphite and $NaNO_3$ were mixed by the weight ratio of 2:1, a certain amount of H_2SO_4 was added to the solution and reacted in a low-temperature environment. Next, add $KMnO_4$ to the solution and control the temperature of the water bath below 35°C. Meanwhile, stirring for 30 minutes until the solution turned brown. Then, the excessed deionized water was added to the mixture to ensure the reaction temperature under 95°C. After stirring for 15 min, 30% H_2O_2 was used to remove excess $KMnO_4$. Finally, the GO suspension was washed repeatedly with 5% HCl and dried at the temperature of 50℃ in a drying oven.

The TAIGO was prepared by the co-blending method. The as-prepared GO, and TA powder was mixed into 100 mL deionized water and reacted in a reflux-stirring device at 80°C. Then, the obtained TAIGO mixture was washed with deionized water several times to remove impurities and finally dried at 90°C.

2.3 Characterization of TAIGO

The Scanning electron microscopy (SEM, HITACHI S-3000N, Japan) was used to observe the morphology of TAIGO. The functional groups on the TAIGO were analyzed by Fourier transform infrared spectroscopy (FTIR, Bruker VERTEX 70, Germany). The Atomic Force Microscope (AFM, Bioscope Resolve, USA) was carried out to observe the structure of TAIGO. The specific surface area (BET, GAPP V-Sorb2800P, China) was also tested to confirm the physic property of GO and TAIGO. Besides, the zeta potential

(Quantachrome DT-300, USA) was measured as an index to revalue the absorbent's surface charge and charge density.

2.4 Adsorption of Hg^{2+} by TAIGO

The adsorption performance evaluation experiments were conducted in the 250 mL conical flask. As depicted in Fig. 1, the adsorption experiments were studied in a stirring apparatus to ensure the reaction was adequate. Then, the absorbent was collected from wastewater by a microfiltration membrane for further use, and the concentration of Hg^{2+} in wastewater was measured by the atomic fluorescence spectrometer (AFS, RGF-6800, China). In this work, the adsorption performance was calculated based on Eq. (1) and Eq. (2). The pH value of wastewater was adjusted by adding a certain amount of HCl and NaOH and measured by a pH meter (VSTAR10, Thermo Fisher Scientific, CHINA).

The amount of Hg^{2+} adsorbed and removal efficiency were based on Eq. (1) and Eq. (2):

$$q_e = \frac{(C_o - C_e)V}{m} \quad (1)$$

$$R = \frac{C_o - C_e}{C_o} \times 100\% \quad (2)$$

Where C_o and C_e (mg/L) represent the initial and equilibrium concentration of Hg^{2+} in wastewater, V (L) is the volume for the solution, and the m (mg) is the weight of the absorbent.

Results And Discussion

3.1 Characterization

The physic-chemical property of GO and TAIGO was confirmed by SEM, AFM and FTIR. The morphology of the TA and TAIGO was shown in Fig. 2. It could be found that the GO and TAIGO exhibited layered structures, which could be accounted for the polar groups on them (Mi et al., 2019). The formation of GO and TAIGO was also determined by AFM in the tapping mode (Fig. 3). It was found that GO showed a height profile of thickness 1 nm, while the TAIGO was 2 nm. The results of AFM indicated that the GO was prepared, and the TA was immobilized on the GO successfully. The immobilization TA could be account for the SN_2 nucleophilic reactions, in which the epoxy ring on GO was destroyed by the phenolic hydroxyl group on TA (Lei et al., 2011). Besides, the π-π interaction and van der Waals force on sites of the aromatic rings were the other possible formation mechanisms (Patil et al., 2009; Li et al., 2010).

To further study the changes in the groups, the FTIR tests were conducted. As shown in Fig. 4, there were many functional groups in GO, such as the hydroxyl groups at 3429 cm^{-1}, carbonyl groups at 1717 cm^{-1} and epoxy groups at 1118 cm^{-1}. With the immobilization of TA, the ring-opening reactions of epoxy groups were getting intense, and the epoxy groups on the TAIGO were significantly weakened. Besides, it

was noticed that the introduction of TA could also be confirmed in the FTIR of TAIGO, in which some characteristic peaks of TA could be observed.

3.2 Adsorption performance

For comparing the difference in removal efficiency between GO and TAIGO, the adsorption experiments in the actual desulfurization wastewater were conducted. In contrast, exhibited in Fig. 5, the removal efficiency of GO and TAIGO in the desulfurization wastewater A was 80.23%, 90.39%, and 65.44%, 78.06% in the desulfurization wastewater B. The TAIGO showed a better adsorption performance than GO, which could be accounted for the inducted abundant of adjacent phenolic hydroxyls on TA. In addition, the results of specific surface area and zeta potential were presented in Table 2, which indicated that the TAIGO exhibited a better pore structure and higher charged properties, which may further enhance the removal performance of Hg^{2+} in wastewater.

Table 2. The specific surface area and zeta potential of GO and TAIGO.

Material	Specific surface area ($m^2 \cdot g^{-1}$)	Zeta potential (mV)
GO	430	-42.8
TAIGO	562	-48.5

Table 3. Kinetic parameters for the adsorption on TAIGO adsorbent.

Pseudo-first-order			Pseudo-second-order		
K_1	q_e (mg/g)	R^2	K_2	q_e (mg/g)	R^2
0.111	10.08	0.691	0.047	23.81	0.9995

3.3 Effect of operation parameters

To better and deeply understand the factors affecting adsorption performance, the simulated desulfurization wastewater prepared by Hg^{2+} solution was used instead of the actual wastewater in the following experiment.

3.3.1 Effect of contact time

Figure 6 showed the effect of reaction time on Hg^{2+} removal efficiency. It could be found that the removal efficiency increased quickly in the initial 10 min and the adsorption process was completed within 15 min. It can be inferred that the adsorption process was rapid, and it took a short time for adsorption completely. The Hg^{2+} concentration in the desulfurization wastewater was relatively high at the initial stage of adsorption, which increased the adsorption driving force. Besides, large amounts of adsorption

sites of TAIGO were available within 15 min. After a period of time, the adsorption sites were occupied, leading to the slow growth in removal efficiency.

3.3.2 Effect of TAIGO dosage

The amount of adsorbent was a vital index for industrial application. The effect of adsorbent dosage was studied by adding different amounts of TAIGO into 250 mL Hg^{2+} containing solution. The reaction time was 120 minutes to ensure the adsorption process proceeded entirely. As shown in Fig. 7, as the dosage of TAIGO increased from 5 mg to 10 mg, the Hg^{2+} removal efficiency increased from 56.28–92.1% and gradually remained stable with the further addition of TAIGO to 20 mg. As the adsorbent addition increased, the adsorption sites of Hg^{2+} gradually increased, which enhanced the binding probability between the TAIGO and Hg^{2+}. However, with the continued increase of the adsorbent dosage, no remarkable variations in removal efficiency were observed. It can be inferred that the adsorption process had reached the saturated state, and the surface of TAIGO adsorption sites was overlapped, which restrict the further improvement in removal efficiency.

3.3.3 Effect of pH

The pH value of the wastewater not only affects the existence of functional groups of the adsorbent but also changes the existence form of Hg^{2+} in the desulfurization wastewater (Wang et al., 2015). Thus, it is essential to investigate the effect of pH on the adsorption performance for Hg^{2+}. In Fig. 8, as the pH value increased from 3 to 12.3, the removal efficiency increased and then decreased. The optimum removal efficiency was obtained at pH of 9. This phenomenon could be ascribed to the following reasons. When the pH value of wastewater was lower than 7, most of the mercury ions in the desulfurization wastewater existed in the valence state of Hg^{2+}, and the excess H^+ ions would bind with the adsorption sites of TAIGO, resulting in a decline in adsorption capacity towards Hg^{2+}. It was noted that the adjacent phenolic hydroxyls on TA were sensitive to the existence of H^+, and the lower pH value was conducive for chelating reaction with Hg^{2+} in desulfurization wastewater (Huang et al., 2009). As the pH value increased to 9, the ionization degree of phenolic hydroxyls located in TA was promoted, leading to the enhancement of the chelation and electrostatic effect between TAIGO and Hg^{2+} (Sun et al., 2020; Ma et al., 2005). However, when the pH value further increased above 9, the Hg^{2+} in the desulfurization wastewater was easily converted into insoluble $Hg(OH)_2$, which was directly related to the decrease of adsorption capacity.

3.3.4 Effect of ion components

To evaluate the adsorption performance of TAIGO in the complex wastewater component, the adsorption experiment in different ion components was conducted. In the actual desulfurization wastewater, the concentration of the Cl^- exhibited a wide range from 4000 to 20000 mg/L, which may affect the adsorptive capacity for Hg^{2+}. The effect of chloride ion (Cl^-) on the adsorption efficiency was shown in Fig. 9 (a). It can be observed that the TAIGO showed an excellent absorption performance (88.2%) at a low concentration of the Cl^- (12000 mg/L). However, as the chloride ions concentration increased, the adsorption efficiency of TAIGO was gradually decreased. It could be ascribed that the excessive chloride

ions in the slurry were likely to accumulate on the surface of TAIGO, leading to a decline in adsorbent surface charge. Besides, it was reported that the Hg^{2+} tended to from $Hg(OH)_2$ to HgCl(OH) and $HgCl_4^{2-}$ in a solution containing chloride ions, and may further hinder the absorption performance (Castro et al., 2011).

Besides, the effect of SO_3^{2-} was also investigated in this work. Although the content of SO_3^{2-} was relatively low in desulfurization wastewater, it may cause the migration and conversion of Hg^{2+} (Wu et al., 2019). Figure 9 (b) gave the effect of concentration of the SO_3^{2-}on removal efficiency. It can be observed that as the concentration of SO_3^{2-} increased to 700 mg/L, the removal efficiency remained at 88.2%. However, when the concentration is more significant than 700 mg/L, the inhibitory effect of SO_3^{2-} on the adsorption efficiency was gradually strengthened, and the adsorption efficiency could be reduced to 75.6%. It was noted that the SO_3^{2-} was an essential factor that caused the Hg^{2+} in the desulfurization wastewater to be reduced to Hg^0 and released into the atmosphere (Ma et al., 2018). Interestingly, with the increase of the SO_3^{2-} concentration, more Hg^{2+} would residue in wastewater. The fact was that the Hg^{2+} would accelerate the free radical reactions, causing the SO_3^{2-} oxidized to SO_4^{2-}. That is, less Hg^{2+} could be involved in the chemical adsorption reaction, which may cause a low adsorption efficiency. Similar results had also been found in other transition metals (Wu et al., 2004). For SO_4^{2-}, as the increase of concentration increased, the removal efficiency showed no remarkable change. It suggested that the existence of SO_4^2 has little impact on removal performance in the desulfurization wastewater system.

In addition, with the development of the desulfurization wastewater concentration technology, the concentrations of Ca^{2+}, Mg^{2+} and Na^+ were in an extensive variation range. Therefore, the effect of Ca^{2+}, Mg^{2+} and Na^+ concentrations was considered, and the results were displayed in Fig. 10. With the concentrations of Ca^{2+}, $Mg^{2+,}$ and Na^+ raised from 2000 to 6000 mg/L, there was no significant decline in the adsorption efficiency. The main reason is that the lack of *d* or *f* electron orbit may cause the weakening of the interaction force between Hg^{2+} and ions. That is, the interaction between Hg^{2+} and TAIGO was stronger than Ca^{2+} and Mg^{2+} ions, and the presence of the Ca^{2+}, Mg^{2+} and Na^+ would not affect the adsorption efficiency of TAIGO (Sun et al., 2014).

3.4 Adsorption kinetics

Adsorption kinetics provided a vital information index about the mechanism of Hg^{2+} adsorption onto TAIGO, which was necessary to depict the adsorption behaviour of TAIGO. In this study, the pseudo-first-order and pseudo-second-order kinetic model was applied to fit the adsorption dates of Hg^{2+} adsorption on the TAIGO.

The pseudo-first-order and pseudo-second-order kinetics model were represented by the following equation:

$$\ln(q_e - q_t) = \ln q_e - k_1 t \quad (3)$$

$$\frac{t}{q_t} = \frac{1}{k_2 q_e^2} + \frac{t}{q_e} \quad (4)$$

Where q_e and q_t (mg/g) represent the amounts of ions adsorbed at equilibrium state and time t (min). The k_1 and k_2 g/(mg·min) are the rate constants of two kinetic models.

Figure 11 shows the fitting curves for the adsorption of Hg^{2+} with TAIGO under natural pH. The correlation coefficient (R^2 = 0.9995) of the pseudo-second-order kinetics model was larger than pseudo-first-order, which indicated that the chemical adsorption played a significant role in the adsorption process of Hg^{2+} and the physical adsorption promoted the adsorption performance (Anbia et al., 2016).

Besides, the parameters k_1 and k_2 were an essential index for evaluating absorbent performance. Table.3 listed the adsorption rate constants based on the pseudo-first-order and pseudo-second-order for Hg^{2+} adsorption. Furthermore, the comparative analysis between TAIGO and other reported GO-based materials was studied. It could be seen from Table 4, and the TAIGO exhibited an excellent absorption performance than most materials and a shorter equilibrium adsorption time needed.

Table 4
Comparison of adsorption capacities with various adsorbents for heavy metals.

Adsorbents	Target pollutant	Kinetic	Adsorption capacity(mg/g)	Equilibrium time (min)	Ref.
Thiol-functionalised silica-coated magnetite	Hg^{2+}	PSO	9.5	15	(Hakami et al., 2012)
EDTA functionalized graphene oxide nanoparticles	Hg^{2+}	PSO	18.6392	160	(Sun et al., 2020)
Magnetic nanoparticle–graphene oxide	Se^{4+}	-	4.99	0.2	(Fu et al., 2014)
Persimmon tannin/graphene oxide composites	Ge^{4+}	-	117.38	-	(Zhang et al., 2019)
Magnetite/reduced graphene oxide nanocomposites	Pb^{2+}	PSO	13.87	180	(Qi et al., 2015)
Tannin-immobilized graphene oxide	Hg^{2+}	PSO	23.81	15	This paper

The probable Hg^{2+} removal mechanism was shown in Fig. 12. For the TAIGO, in desulfurization wastewater, the considerable surface area of GO was acting as a large net to capture the Hg^{2+} and served as the carriers for TA. Also, the functional groups in GO could improve the removal performance for Hg^{2+}. Besides, the multiple ortho-position phenolic hydroxyl structure of TA functioned as a multi-base ligand to complex reaction with Hg^{2+}. A stable five-membered ring chelate with Hg^{2+} was formed, which was the

form of oxygen anions. The third phenolic hydroxyl group in the pyrogallol structure could further promoted the dissociation effect of the other two phenolic hydroxyl groups. Thus, the stability of Hg^{2+} based complexes could be formed, and the Hg^{2+} was effectively removed from desulfurization wastewater.

3.5 Regeneration performance

The regeneration performance was a crucial factor in evaluating the absorbent's economics, so it is necessary to conduct the regeneration experiment. In this experiment, a strongly acidic environment was created to complete the regeneration process, the 0.1 mol/L HCl was applied to elute the absorbent. In Fig. 13, the removal efficiency has remained at 88% after three recycles. As discussed in the effect of pH, the excess H^+ would lead to the protonated effect on TAIGO, the Hg^{2+} would be replaced, and excellent desorption efficiency could be achieved. However, the decomposition of adsorbents would occur in the process elute, leading to a slight efficiency decline in the third absorption that the pristine one. The good regeneration performance of TAIGO indicated that it was an economical and efficient absorbent, which could be further used in the practical desulfurization wastewater.

Conclusion

In this work, a novel adsorbent based on tannin-immobilized graphene oxide was proposed, and the adsorption performance of was TAIGO evaluated under different conditions. The prepared TAIGO exhibited an excellent adsorption performance for Hg^{2+} in desulfurization wastewater, attributing to the functional groups in GO and TA. The adsorption process fits well with the pseudo-second-order kinetic model. Besides, the removal efficiencies of Hg^{2+} were influenced by many factors, such as the contact time, adsorbent dosage, pH and ion components. The experimental results showed that the adsorption process would complete within 15 min, and the removal efficiency would enhance by increased adsorbent dosage. The pH value would affect the protonation process of TAIGO and the form of Hg^{2+} in the wastewater. The optimum removal efficiency was obtained at pH of 9. For the ion component, the high-concertation Cl^- and SO_3^{2-} would hinder the absorption performance, while SO_4^{2-} and cations have a negligible impact. Besides, an excellent economic benefit of TAIGO was achieved in the regeneration performance evaluation experiment, indicating that the TAIGO was a cost-effective method, which could be further used in the practical desulfurization wastewater.

Declarations

Ethical Approval

Not applicable

Consent to Participate

Not applicable

Consent to Publish

Not applicable

Authors Contributions

Heng Chen: Conceptualization, Methodology, Formal analysis, Investigation, Resources, Writing Original Draft, Writing - Review & Editing.

Fengjun Liu: Methodology, Investigation, Review & Editing.

Chenjian Cai: Methodology, Resources, Writing - Review & Editing.

Hao Wu: Conceptualization, Writing - Review & Editing, Supervision.

Linjun Yang: Conceptualization, Writing - Review & Editing, Supervision.

Funding

The project was financially supported by the National Natural Science Foundation of China (52076046, 51806107).

Competing Interests

The authors declare that they have no competing interests.

Availability of data and materials

All data generated or analysed during this study are included in this published article.

Acknowledgements

The project was financially supported by the National Natural Science Foundation of China (52076046, 51806107).

References

1. Anbia M., Amirmahmoodi S. Removal of Hg(II) and Mn(II) from aqueous solution using nanoporous carbon impregnated with surfactants. Arab. J. Chem. 9, S319-S325. https://doi.org/10.1016/j.arabjc.2011.04.004
2. Bao J., Fu Y., Bao Z.H. Thiol-functionalized magnetite/graphene oxide hybrid as a reusable adsorbent for Hg^{2+} removal. Nanoscale Res. Lett. 8(1), 486. https://doi.org/10.1186/1556-276X-8-486
3. Castro L., Dommergue A., Renard A., Ferrari C., Ramírez-Solís A., Maron L. Theoretical study of the solvation of $HgCl_2$, HgClOH, $Hg(OH)_2$ and $HgCl_3^-$: A density functional theory cluster approach. PCCP. 13, 16772-16779. https://doi.org/10.1039/C1CP22154J

4. Chang L., Zhao Y.C., Li H., Tian C., Zhang Y., Yu X.H., Zhang J.Y. Effect of sulfite on divalent mercury reduction and re-emission in a simulated desulfurization aqueous solution. Fuel Process. Technol. 165, 138-144. https://doi.org/10.1016/j.fuproc.2017.05.016
5. Ebrahim M., Sepehr A., Abdul W.M., Law Y.N., Abdelbaki B., Wei L.A., Muneer B.,Simultaneous removal of Congo red and cadmium(II) from aqueous solutions using graphene oxide–silica composite as a multifunctional adsorbent, Journal of Environmental Sciences, 98, 151-160. https://doi.org/10.1016/j.jes.2020.05.013.
6. Fan R.Y., Min H.Y., Hong X.X., Yi Q.P., Liu W., Zhang Q.L., Luo Z.R. Plant tannin immobilized Fe_3O_4@SiO_2 microspheres: A novel and green magnetic bio-sorbent with superior adsorption capacities for gold and palladium. J. Hazard. Mater. 364(15), 780-790. https://doi.org/10.1016/j.jhazmat.2018.05.061
7. Fu Y., Wang J.Y., Liu Q.X., Zeng H.B. Water-dispersible magnetic nanoparticle–graphene oxide composites for selenium removal. Carbon. 77, 710-721. https://doi.org/10.1016/j.carbon.2014.05.076
8. Hakami O., Zhang Y., Banks C.J. Thiol-functionalised mesoporous silica-coated magnetite nanoparticles for high efficiency removal and recovery of Hg from water. J. Water. Re. 46(12), 3913-3922. https://doi.org/10.1016/j.watres.2012.04.032
9. Hsu C.J., Chen Y.H., Hsi H.C. Adsorption of aqueous Hg^{2+} and inhibition of Hg^0 re-emission from actual seawater flue gas desulfurization wastewater by using sulfurized activated carbon and NaClO. Sci. Total. Environ. 711(1), 135172. https://doi.org/10.1016/j.scitotenv.2019.135172
10. Huang X., Liao X.P., Shi B. Hg(II) removal from aqueous solution by bayberry tannin-immobilized collagen fiber. J. Hazard. Mater. 170(2), 1141-1148. https://doi.org/10.1016/j.jhazmat.2009.05.086
11. Jan B., Marcinowski P., Majewski M., Zawadzki J., Sivakumar S. Alternative Approach to Current EU BAT Recommendation for Coal-Fired Power Plant Flue Gas Desulfurization Wastewater Treatment. Processes. 6(11), 229. https://doi.org/10.3390/pr6110229
12. Krzyżyńska R., Szeliga Z., Pilar L., Borovec K. High mercury emission (both forms: Hg^0 and Hg^{2+}) from the wet scrubber in a full-scale lignite-fired power plant. Fuel. 270(15), 117491. https://doi.org/10.1016/j.fuel.2020.117491
13. Lei Y.D., Tang Z.H., Liao R.J., Guo B.C. Hydrolysable tannin as environmentally friendly reducer and stabilizer for graphene oxide. Green Chem. 13(7), 1655-1658. https://doi.org/10.1039/C1GC15081B
14. Li M., Wang B., Yang M.Q. Promoting mercury removal from desulfurization slurry via S-doped carbon nitride/graphene oxide 3D hierarchical framework. Sep. Purif. Technol. 239(15), 116515. https://doi.org/10.1016/j.seppur.2020.116515
15. Li F.H., Bao Y., Chai J., Zhang Q.X., Han D.X., Niu L. Synthesis and Application of Widely Soluble Graphene Sheets. Langmuir. 26(14), 12314-12320. https://doi.org/10.1021/la101534n
16. Ma H.W., Liao X.P., Liu X., Shi B. Recovery of platinum(IV) and palladium(II) by bayberry tannin immobilized collagen fiber membrane from water solution. J. Membr. Sci. 278(1), 373-380. https://doi.org/10.1016/j.memsci.2005.11.022

17. Ma S.C., Chai J., Wu K., Wan Z.S., Xiang Y.J., Zhang J.R., Fan Z.X. Experimental and mechanism research on volatilization characteristics of HCl in desulfurization wastewater evaporation process using high temperature flue gas. J. Ind. Eng. Chem. 66(25), 311-317. https://doi.org/10.1016/j.jiec.2018.05.045
18. Mi X., Huang G.B., Xie W.S., Wang W., Liu Y. Preparation of graphene oxide aerogel and its adsorption for Cu^{2+} ions. Carbon. 50(13), 4856-4864. https://doi.org/10.1016/j.carbon.2012.06.013
19. Mounir G., Kais D., Soumya C., Anouar H. Enhanced photocatalytic activities of silicon nanowires/graphene oxide nanocomposite: Effect of etching parameters, J. Environ. Sci. 101, 123-134. https://doi.org/10.1016/j.jes.2020.08.010.
20. Palanivel B., Murugaiyan V., Marimuthu S. Synthesis and characterization of GO/$FeSO_4$ composites for the effective removal of Hg^{2+} and Cd^{2+} ions from the synthetic effluent. Environ. Sci. Pollut. R. 27(17), 20621-20628. https://doi.org/10.1007/s11356-019-05994-2
21. Patil A.J., Vickery J.L., Scott T.B., Mann S. Aqueous Stabilization and Self-Assembly of Graphene Sheets into Layered Bio-Nanocomposites using DNA. Adv. Mater. 21(13), 3159-3164. https://doi.org/10.1002/adma.200803633
22. Powell C., Beall G.W. Graphene oxide and graphene from low grade coal: Synthesis, characterization and applications. Opin. Colloid. In. 20(5), 362-366. https://doi.org/10.1016/j.cocis.2015.11.003
23. Qi T., Huang C.C., Yan S., Li X.J., Pan S.Y. Synthesis, characterization and adsorption properties of magnetite/reduced graphene oxide nanocomposites. Talanta. 144, 1116-11124. https://doi.org/10.1016/j.talanta.2015.07.089
24. Sun J.X., Chen H., Qi D.X., Wu H., Zhou C.S., Yang H.M. Enhanced immobilization of mercury(II) from desulphurization wastewater by EDTA functionalized graphene oxide nanoparticles. Environ. Technol. 41(11), 1366-1379. https://doi.org/10.1080/09593330.2018.1534893
25. Sun P.Z., Zheng F., Zhu M., Song Z.G. Selective Trans-Membrane Transport of Alkali and Alkaline Earth Cations through Graphene Oxide Membranes Based on Cation-π Interactions. ACS Nano. 8(1), 850-859. https://doi.org/10.1021/nn4055682
26. Taksitta K., Sujarit P., Ratanawimarnwong N., Donpudsa S.C., Songsrirote K. Development of tannin-immobilized cellulose fiber extracted from coconut husk and the application as a biosorbent to remove heavy metal ions. Environ. Nanotechnol. Monit. Manage. 14, 100389. https://doi.org/10.1016/j.enmm.2020.100389
27. Taurozzi J.S., Redko M.Y., Manes K.M., Jackson J.E., Tarabara V.V. Microsized particles of Aza222 polymer as a regenerable ultrahigh affinity sorbent for the removal of mercury from aqueous solutions. Sep. Purif. Technol. 116(15), 415–425. https://doi.org/10.1016/j.seppur.2013.06.005
28. Wang Z.M., Gao M.M., Li X.J., Ning J.L. Efficient adsorption of methylene blue from aqueous solution by graphene oxide modified persimmon tannins. Sci. Eng. Compos. Mater. 108, 110196. https://doi.org/10.1016/j.msec.2019.110196
29. Wang Y.G., Shi L., Gao L., Wei Q., Cui L., Hu M. The removal of lead ions from aqueous solution by using magnetic hydroxypropyl chitosan/oxidized multiwalled carbon nanotubes composites. J.

Colloid Interface Sci. 451(1), 7-14. https://doi.org/10.1016/j.jcis.2015.03.048

30. Wu H., Chen H., Wang Q.W., Yang H.M. Characteristics and inhibition of mercury re-emission from desulfurization slurry by Fenton reagent. Fuel Process. Technol. 188(1), 89-97. https://doi.org/10.1016/j.fuproc.2019.02.006
31. Wu X.Q., Wu Z.B., Wang D.H. Catalytic oxidation of calcium sulfite in solution/aqueous slurry. J. Environ. Sci. 16(6), 973-977. https://doi.org/10.3321/j.issn:1001-0742.2004.06.020
32. Yang S.L., Sha S.M., Lu H., Wu J.D., Ma J.F., Wang D.W., Hou C.P., Sheng Z.L. Graphene oxide and reduced graphene oxide coated cotton fabrics with opposite wettability for continuous oil/water separation. Sep. Purif. Technol. 259(15), 118095. https://doi.org/10.1016/j.seppur.2020.118095
33. Yue T., Liu Z.Y., Yao K., Song W.B., Sun Y.J., Wang H.L., Xu Y.H. Preparation of Attapulgite/$CoFe_2O_4$ Magnetic Composites for Efficient Adsorption of Tannic Acid from Aqueous Solution. Int. J. Environ. Res. Public. Health. 16(12), 2187. https://doi.org/10.3390/ijerph16122187
34. Zhang Y.Y., Li X.Z., Gong L.F., Xing Z.Q., Lou Z.Q. Persimmon tannin/graphene oxide composites: Fabrication and superior adsorption of germanium ions in aqueous solution. J. Taiwan Inst. Chem. E. 104, 310-317. https://doi.org/10.1016/j.jtice.2019.08.024
35. Zheng C.H., Zheng H., Yang Z.D. Experimental study on the evaporation and chlorine migration of desulfurization wastewater in flue gas. Environ. Sci. Pollut. R. 26, 4791–4800. https://doi.org/10.1007/s11356-018-3816-y
36. Zheng L.B., Jiao Y.Y., Zhong H., Zhuang C., Wang J., Wei Y.S. Insight into the magnetic lime coagulation-membrane distillation process for desulfurization wastewater treatment: From pollutant removal feature to membrane fouling. J. Hazard. Mater. 391(5), 122202. https://doi.org/10.1016/j.jhazmat.2020.122202

Figures

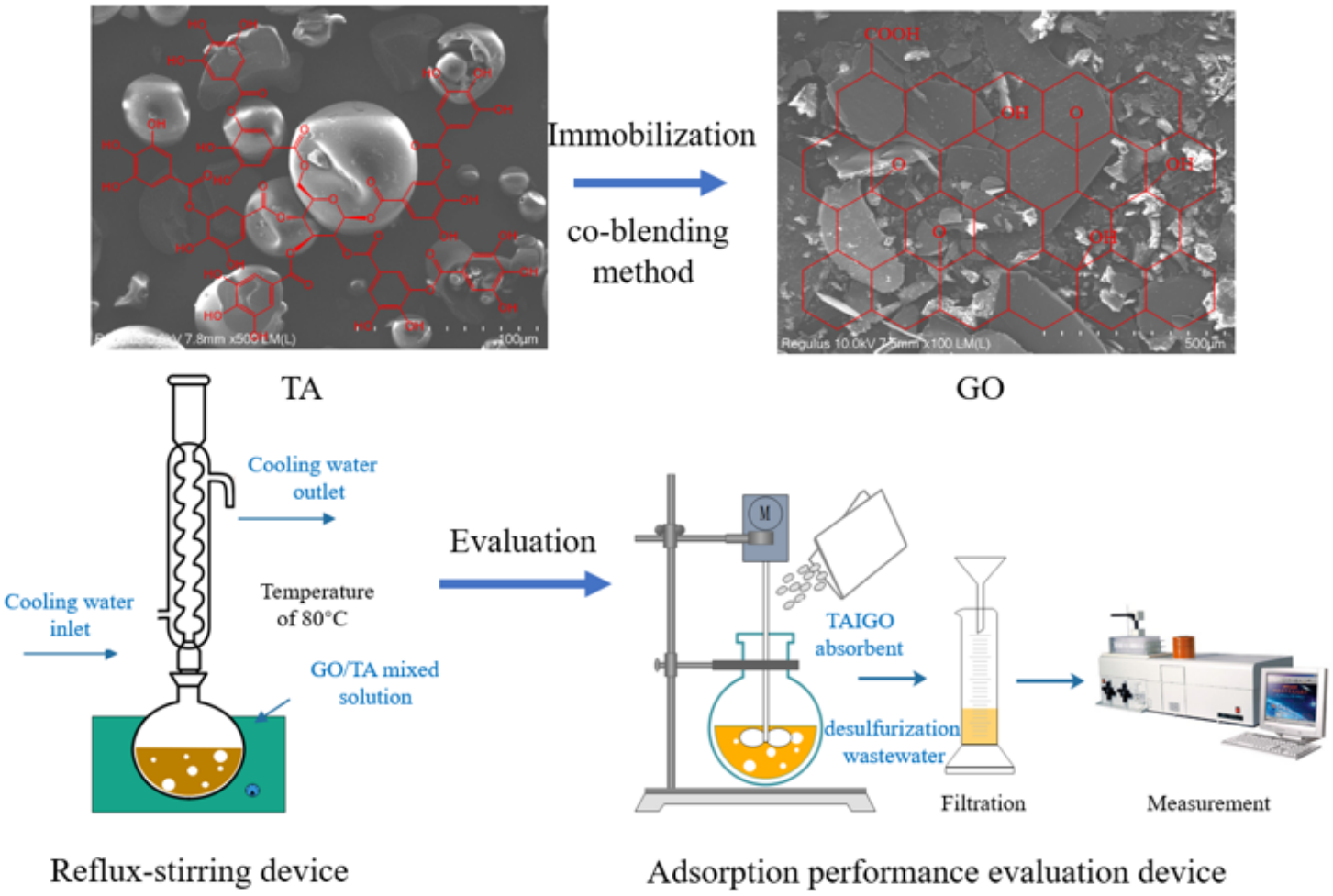

Figure 1

Diagram of the experimental device.

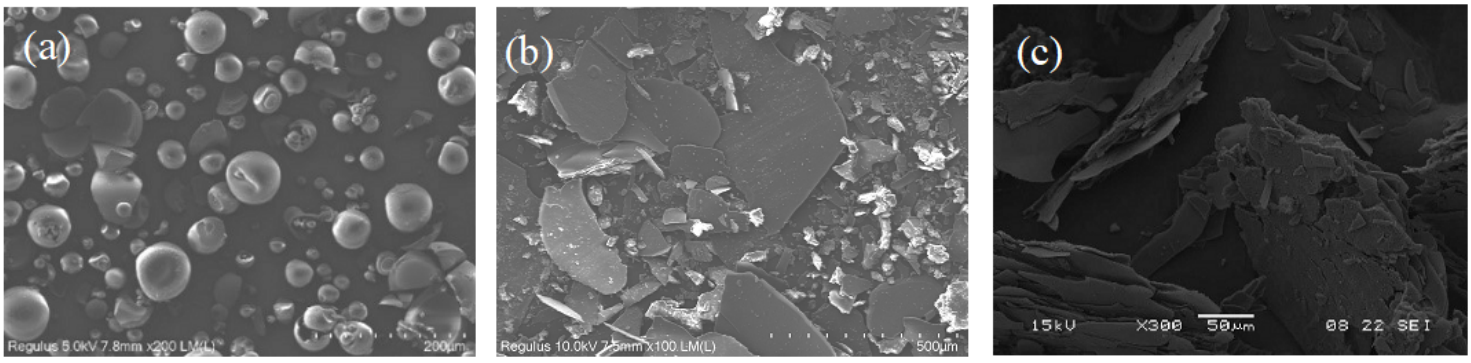

Figure 2

SEM images of GO and TAIGO.

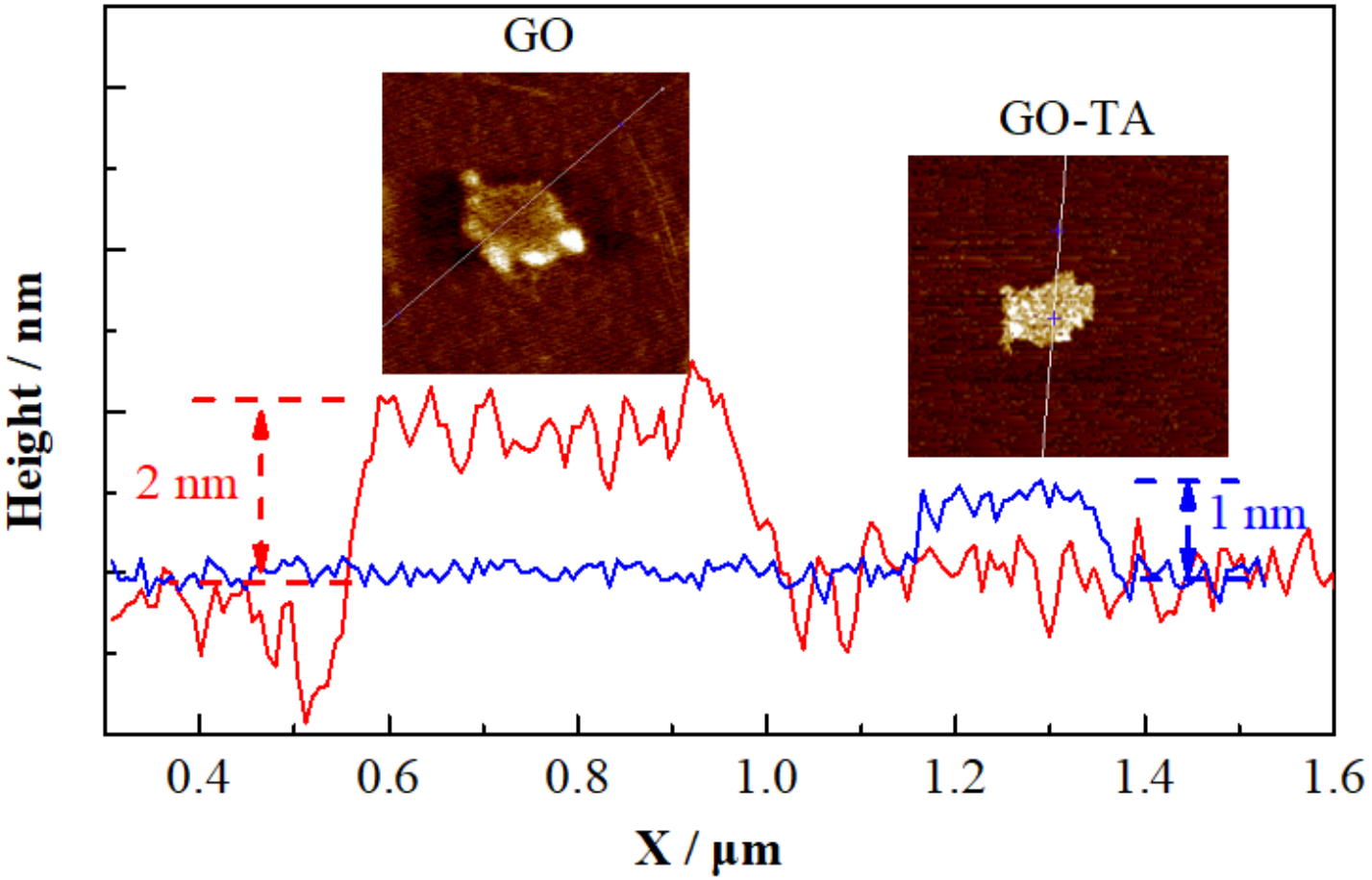

Figure 3

The AFM image of GO and TAIGO.

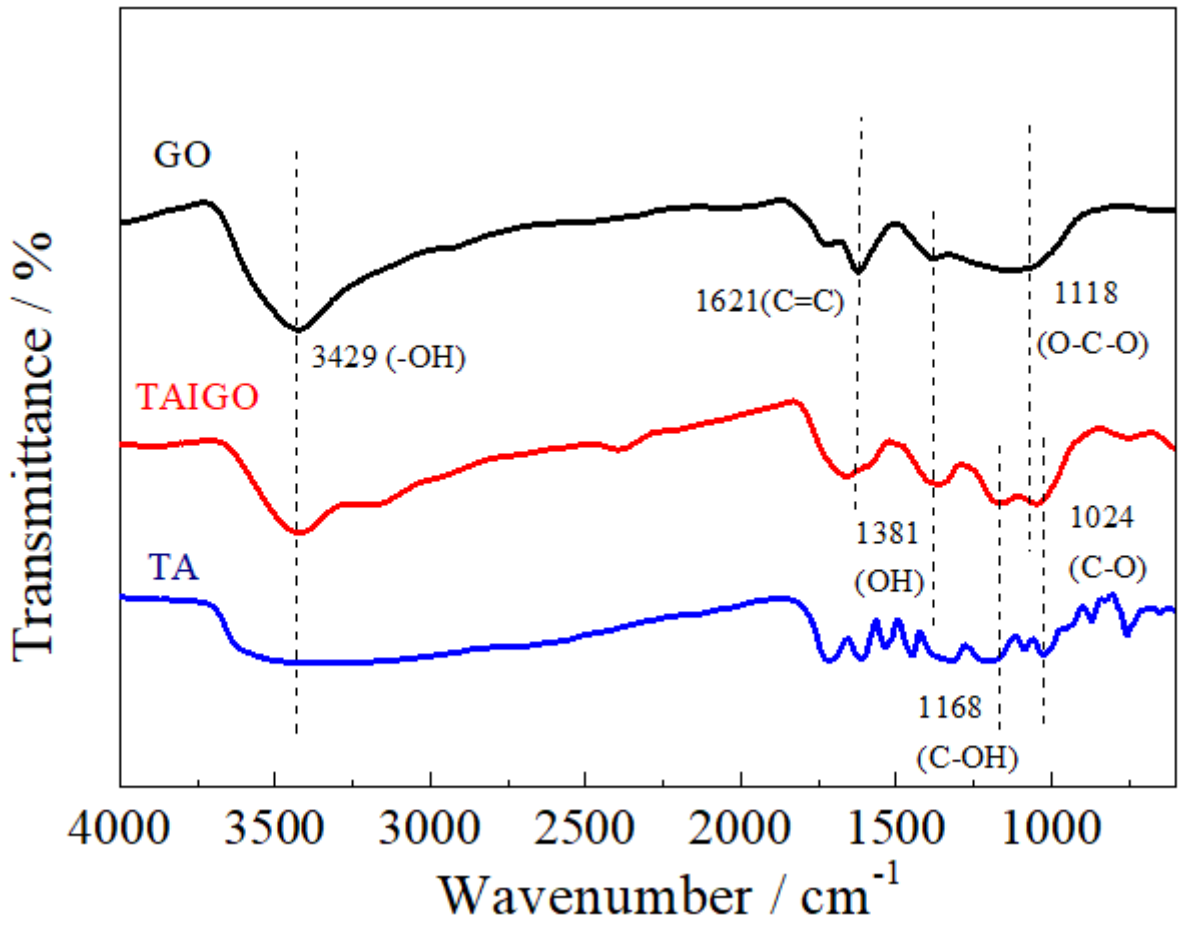

Figure 4

The FTIR spectra of GO, TAIGO and TA.

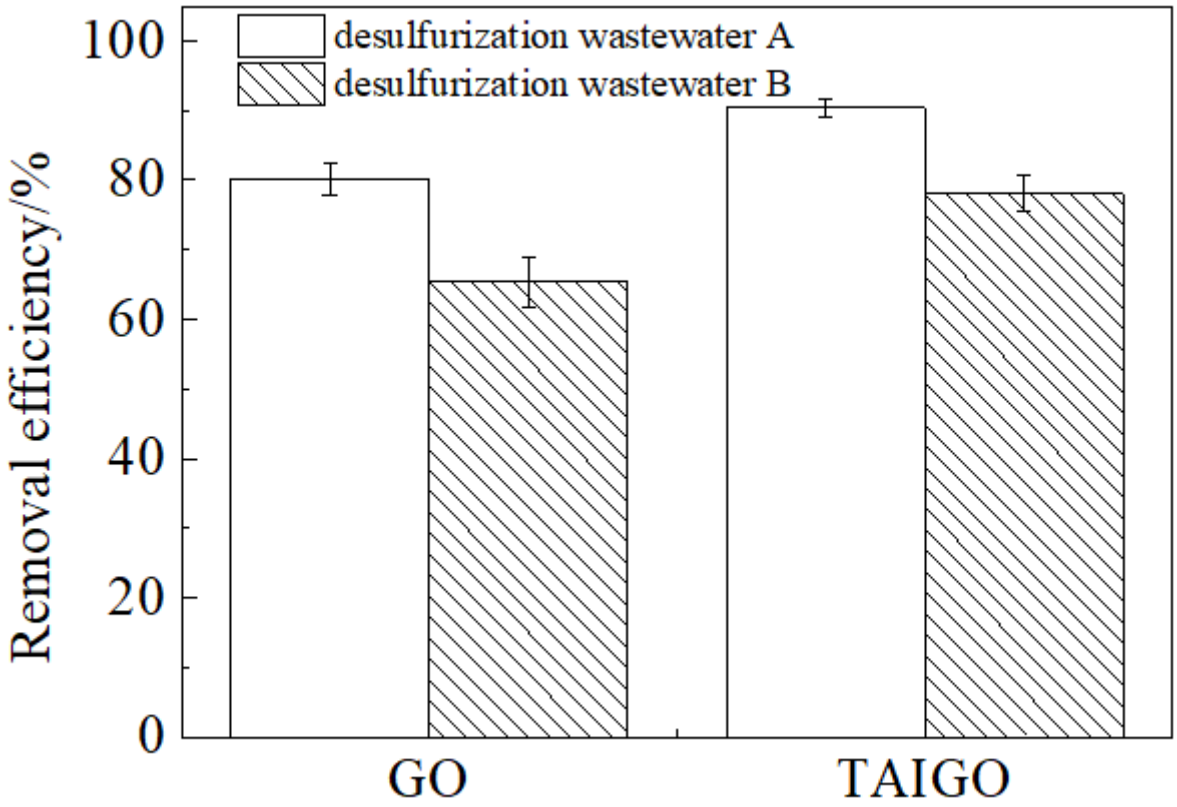

Figure 5

Removal efficiency of GO and TAIGO on Hg2+ in the desulfurization wastewater. (m=40 mg, V=0.25 L, reaction time=120 minutes)

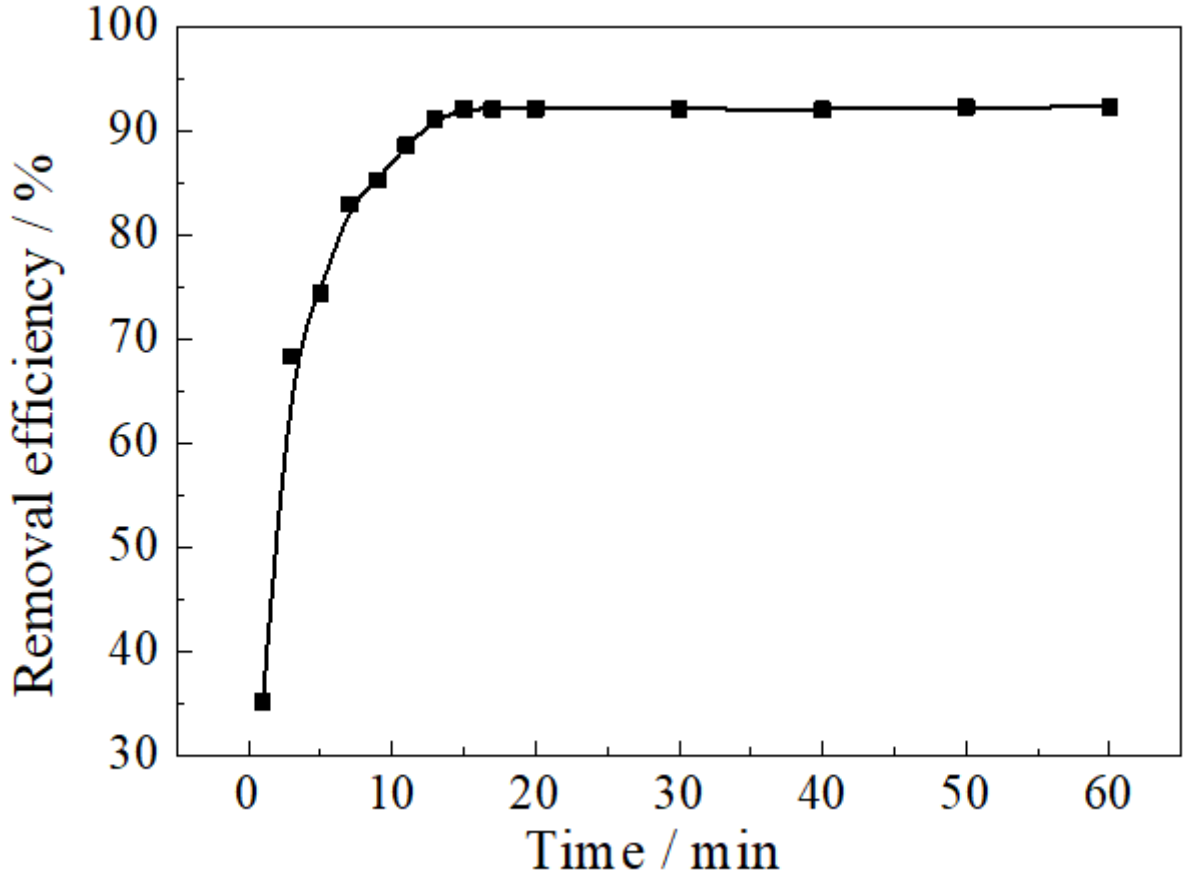

Figure 6

Effect of reaction time on removal efficiency. (C0=1 mg/L, V=0.25 L, natural pH, m=10 mg)

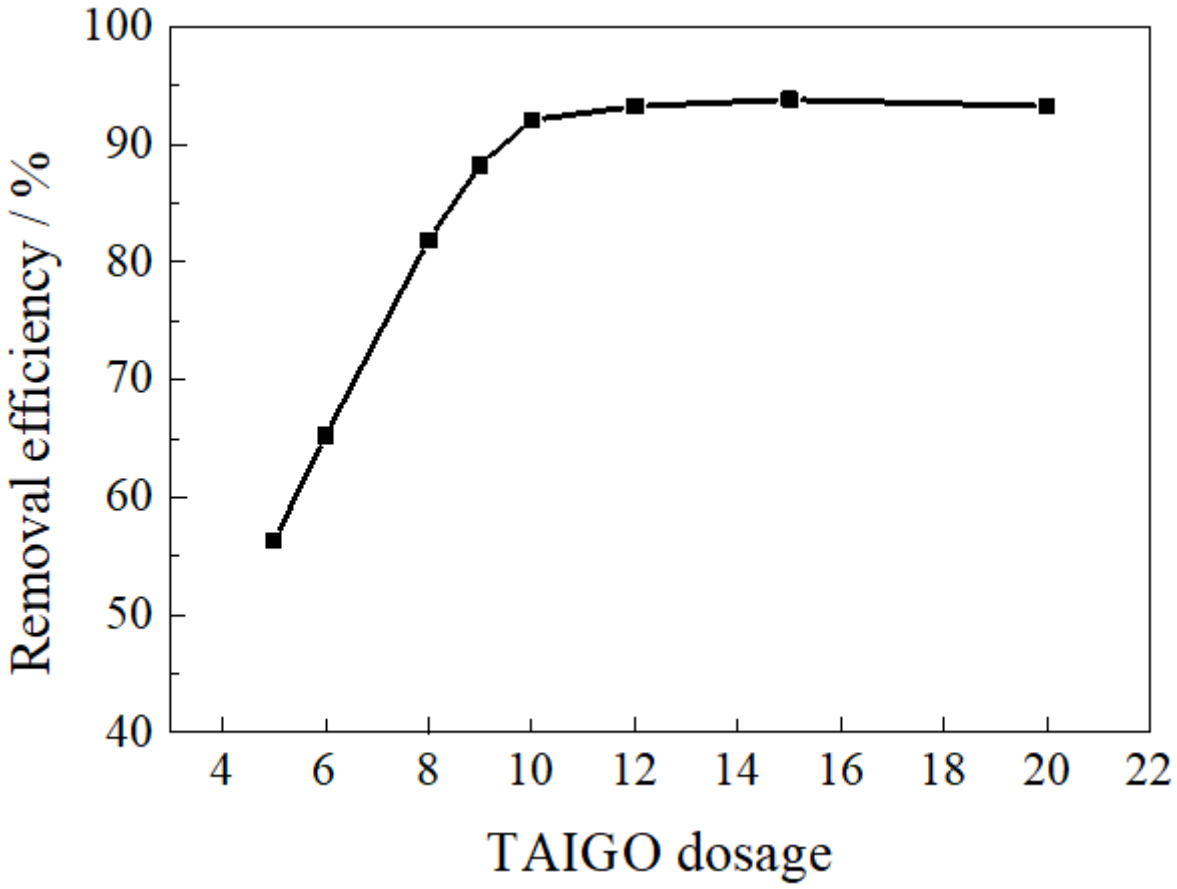

Figure 7

Effect of TAIGO dosage on removal efficiency (C0=1 mg/L, V=0.25 L, natural pH, reaction time=120 minutes)

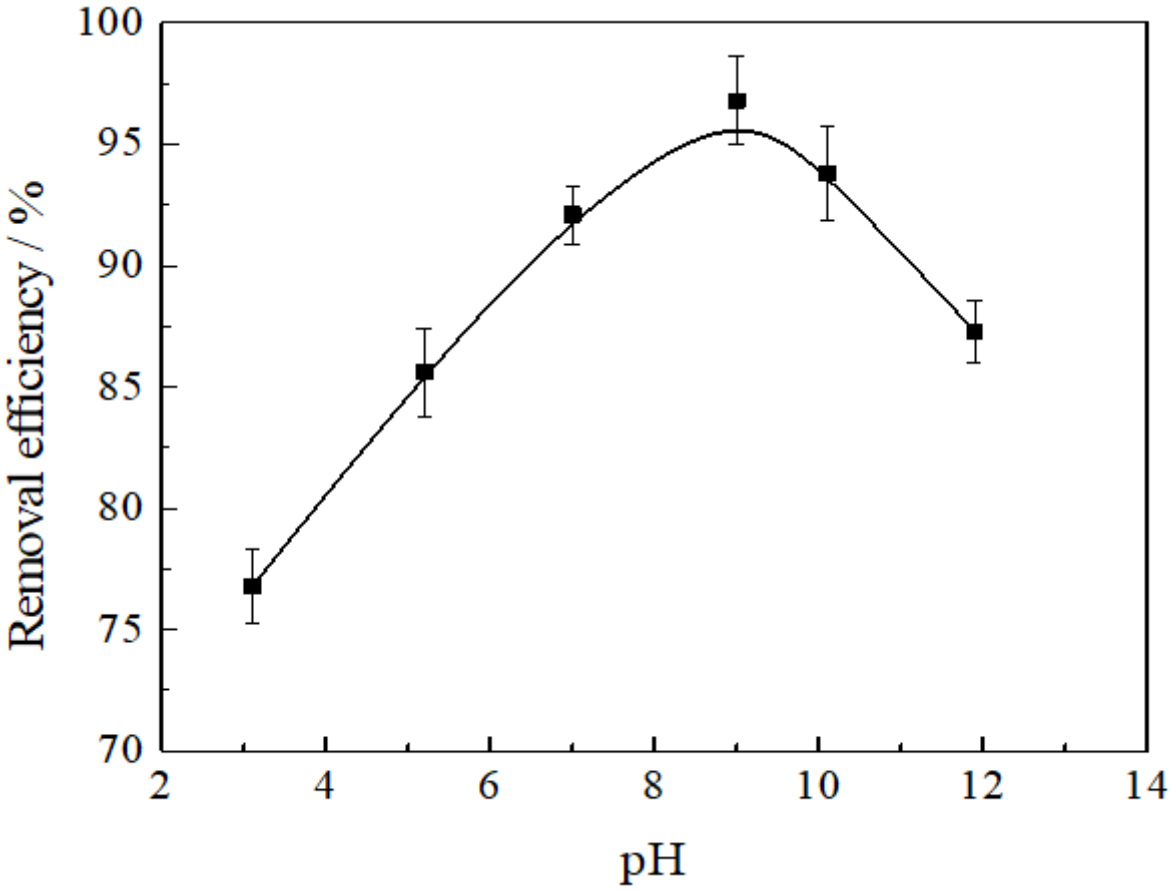

Figure 8

Effect of pH value on removal efficiency. (C0=1 mg/L, V=0.25 L, m=10 mg, reaction time=120 minutes)

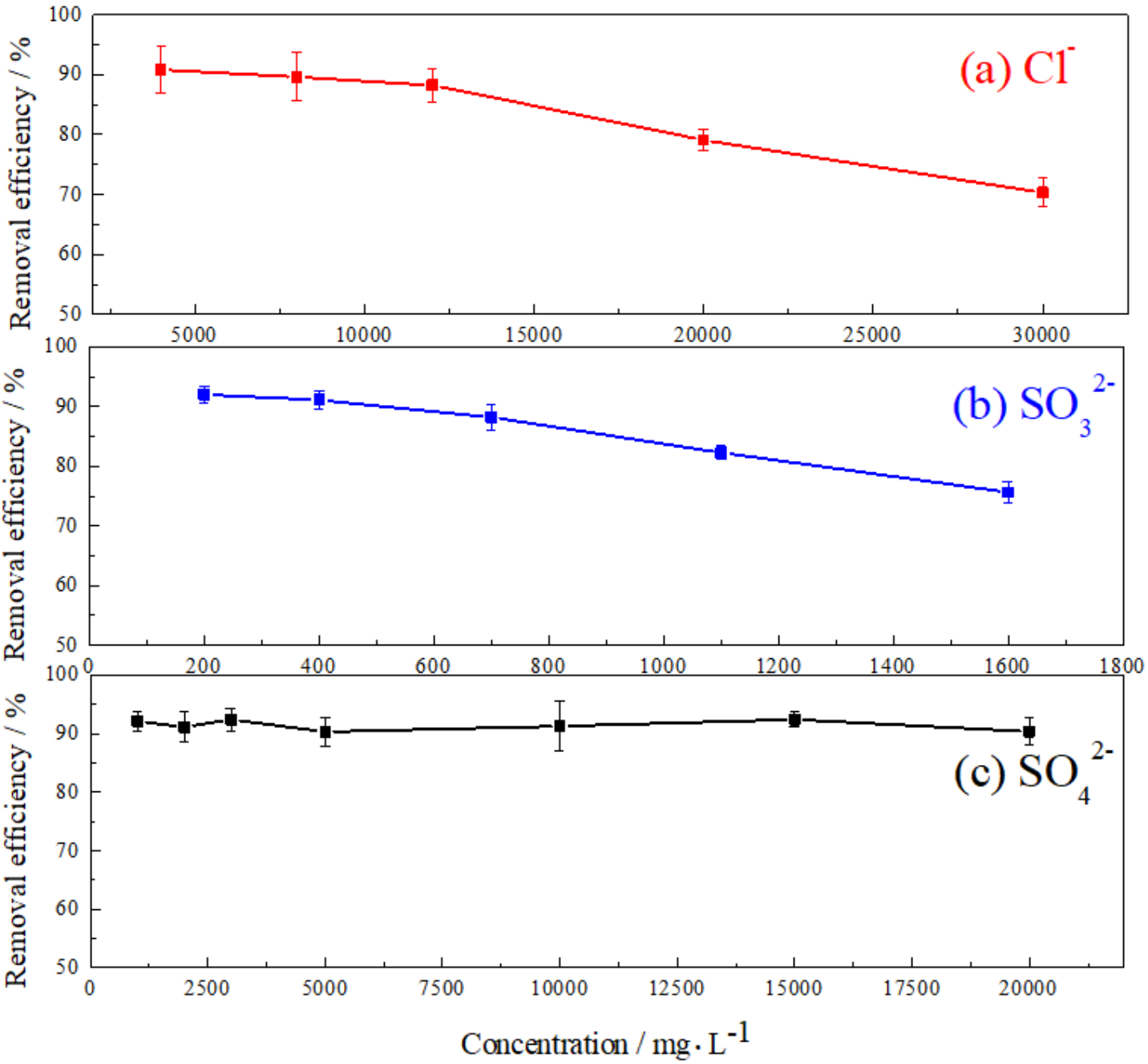

Figure 9

Effect of anions component on removal efficiency. (C0=1 mg/L, V=0.25 L, m=10 mg, natural pH, reaction time=120 minutes)

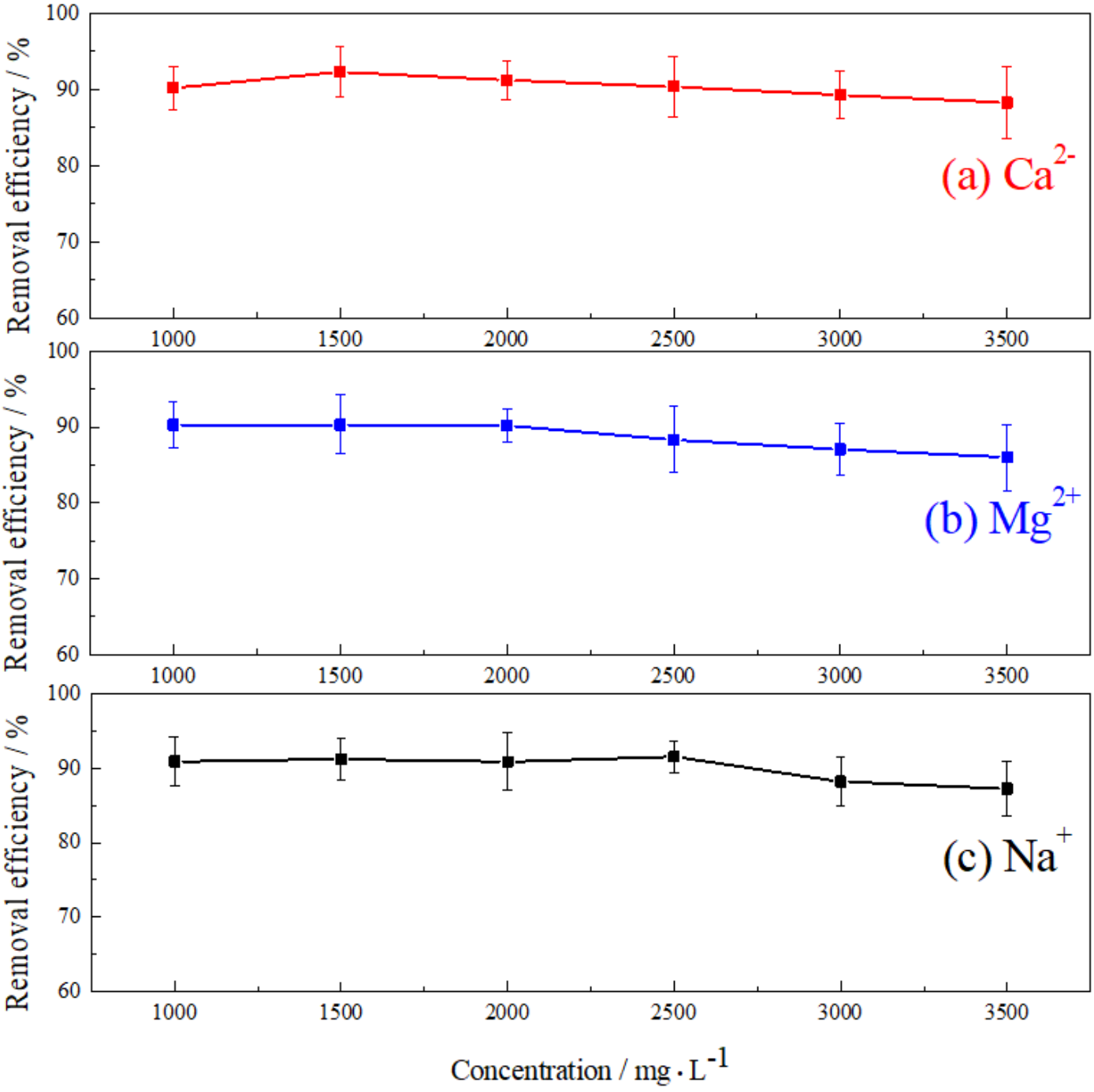

Figure 10

Effect of cations component on removal efficiency. (C0=1 mg/L, V=0.25 L, m=10 mg, natural pH, reaction time=120 minutes)

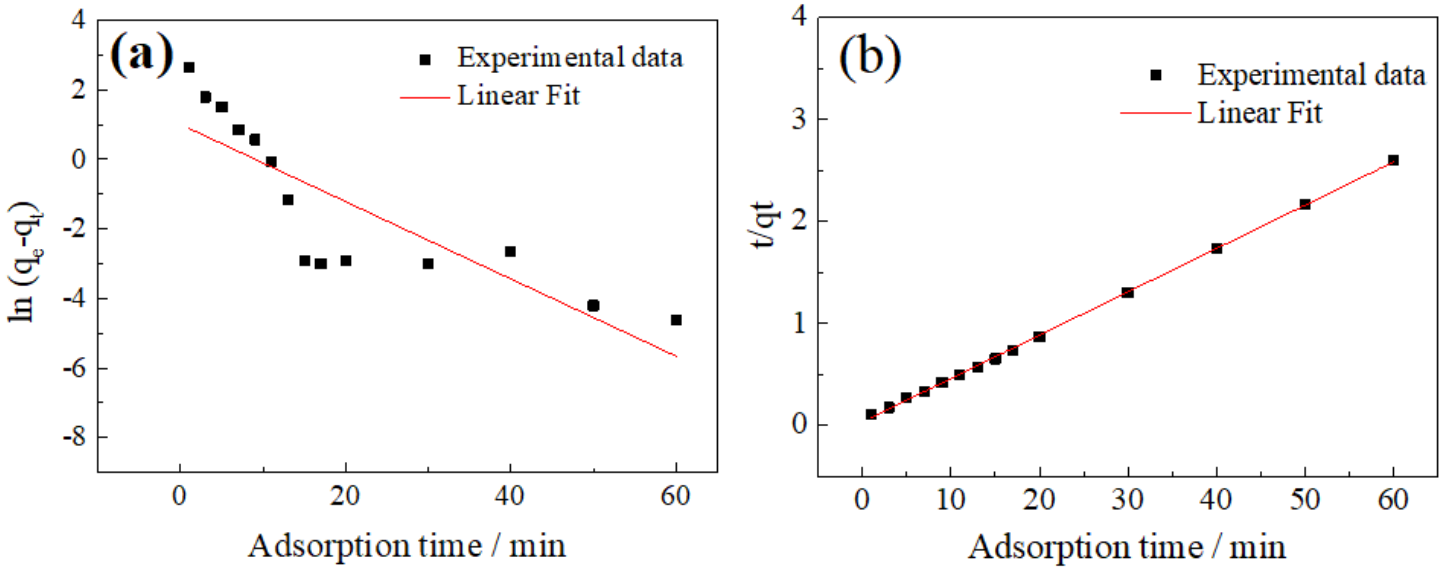

Figure 11

The kinetic models fitting (a) the pseudo-first-order model (b) the pseudo-second-order model.

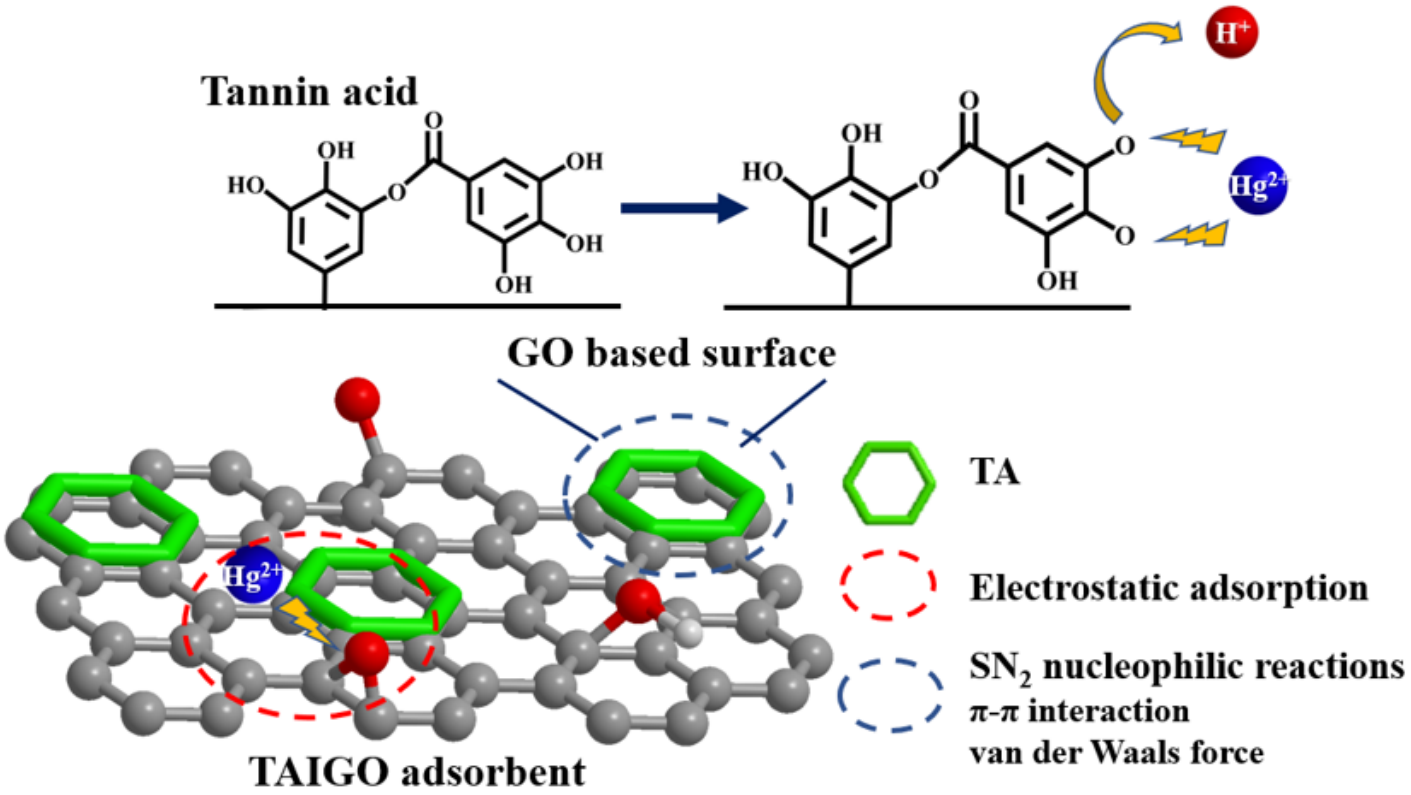

Figure 12

The probable Hg2+ removal mechanism.

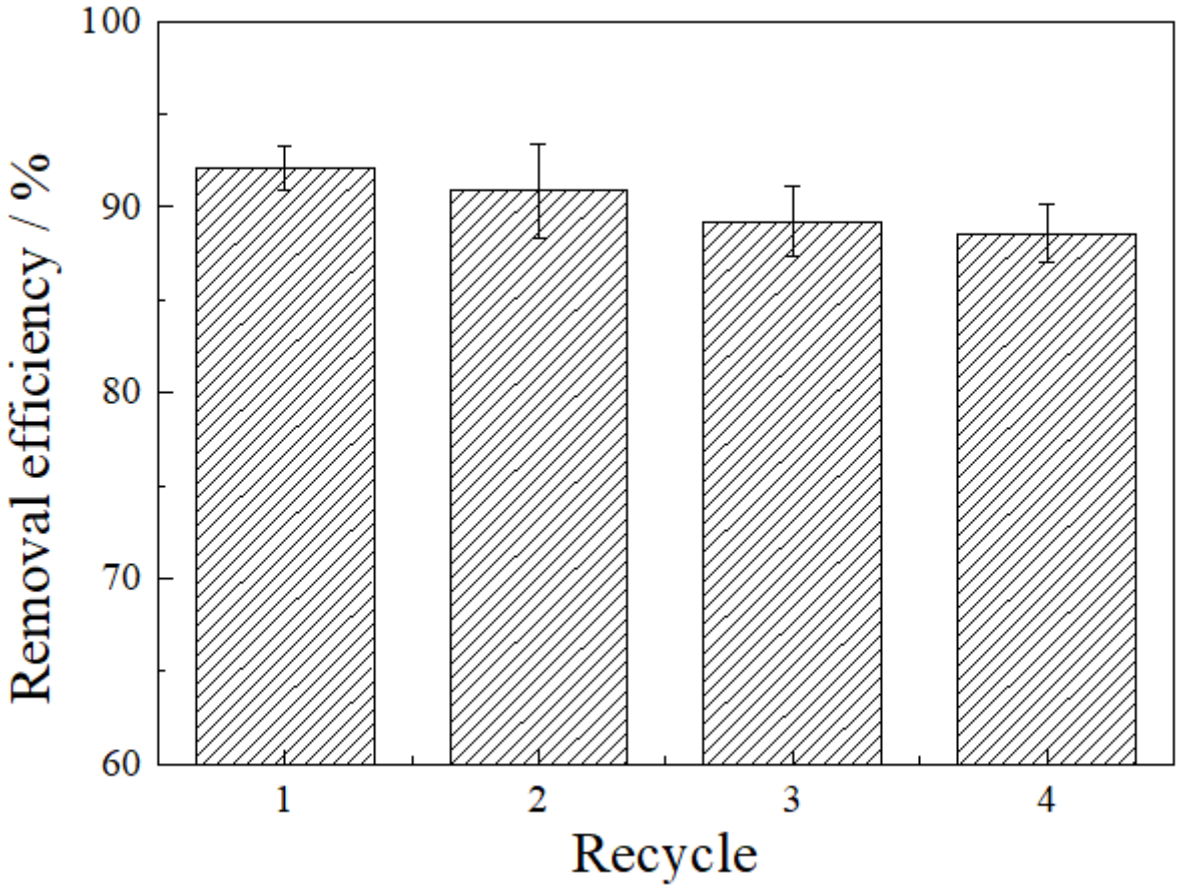

Figure 13

The regeneration performance of TAIGO. (C0=1 mg/L, V=0.25 L, m=10 mg, natural pH, reaction time=120 minutes, eluted by HCl)

Supplementary Files

This is a list of supplementary files associated with this preprint. Click to download.

- GraphicalAbstract.png